

# Role of Diffusion-Weighted MR Imaging in Differentiation of Infectious Spondylodiscitis and Spinal Malignancy

Theeraphol Panyaping MD<sup>1</sup>, Supika Wansophonkul MD<sup>1</sup>, Lojana Tuntiyatorn MD<sup>1</sup>

<sup>1</sup> Department of Diagnostic and Therapeutic Radiology, Faculty of Medicine, Ramathibodi Hospital, Mahidol University, Bangkok, Thailand

**Objective:** To compare apparent diffusion coefficient [ADC] values between infectious spondylodiscitis and spinal malignant tumors. In addition, to determine sensitivity, specificity, accuracy, positive predictive value [PPV], and negative predictive value [NPV] using ADC value cutoff point for diagnosis of infectious spondylodiscitis.

**Materials and Methods:** Eighteen patients with 53 vertebral marrow lesions of suspected infectious spondylodiscitis or spinal malignant tumors acquired between March 2015 and March 2016 were prospectively performed diffusion-weighted MR imaging with ADC mapping. The authors measured the minimal ADC values [min ADC], mean ADC values [mean ADC] and maximal ADC values [max ADC] of the enhancing lesions or hyperintense T2 marrow lesions. These parameters were compared between infectious spondylodiscitis and spinal malignant tumors to find the ADC value cutoff point for diagnosis of infectious spondylodiscitis.

**Results:** The mean ADC values of the infectious spondylodiscitis were found to be significantly higher than those of the spinal malignant tumors,  $1.30 \pm 0.28 \times 10^{-3} \text{ mm}^2/\text{second}$  and  $1.10 \pm 0.20 \times 10^{-3} \text{ mm}^2/\text{second}$ , respectively. Sensitivity, specificity, accuracy, PPV, and NPV of the diagnosis of infectious spondylodiscitis using mean ADC value cutoff points of  $1.116 \times 10^{-3} \text{ mm}^2/\text{second}$  were 75%, 68%, 71.7%, 72.4%, and 70.8%, respectively.

**Conclusion:** Diffusion-weighted MR imaging has a role in differentiating between infectious spondylodiscitis and spinal malignant tumors, especially when imaging findings on conventional images are inconclusive.

**Keywords:** MRI, DWI, ADC value, Infectious spondylodiscitis, Spinal malignant tumors

J Med Assoc Thai 2018; 101 (3): 351-60

Website: <http://www.jmatonline.com>

Infectious spondylodiscitis can affect a wide range of patients and may have a subtle clinical course, with difficulty in diagnosis. Mortality rates of vertebral osteomyelitis have been reported in a range of 2% to 20%<sup>(1,2)</sup>. Early diagnosis of infectious spondylodiscitis is important for appropriate treatment, resulting in good clinical outcomes. Magnetic resonance imaging [MRI] is the most sensitive (93% to 96%) and specific (92.5% to 97%) modality for early detection of spondylodiscitis<sup>(3)</sup>. Typical MRI findings in the infectious spondylodiscitis are low signal on T1-weighted, and high signal on T2-weighted MR images with enhancement on post-contrast T1-weighted images of the affected vertebral bodies, high signal on T2-weighted MR images with loss of intranuclear cleft and peripheral enhancement of the involved disk<sup>(4)</sup>. On the other hand, the morphologic criteria that favor spinal malignant tumors are paravertebral soft tissue masses, involvement of the posterior

elements, and irregularity of the posterior vertebral margin<sup>(5,6)</sup>. Although the conventional MRI is useful in detection and to determine extension of these diseases, the imaging findings of infectious spondylodiscitis and spinal malignant tumors can mimic each other. A conclusive diagnosis requires biopsy and culture, which are invasive and not always definitive. The previous study on 1.5-T diffusion-weighted MR has shown that diffusion-weighted imaging [DWI] and apparent diffusion coefficient [ADC] value may help to differentiate these lesions<sup>(7)</sup>. The mean ADC value of infectious paraspinal masses was significantly higher than that of malignant soft-tissue masses. Many previous studies have used DWI techniques that allow for the calculation of ADC values, showing significant difference of ADC values between pathologic and benign compression fractures using 1-T or 1.5-T MRI<sup>(8-11)</sup>.

To our best knowledge, there has not been any study on 3-T diffusion-weighted MR technique in differentiating between infectious spondylodiscitis and spinal malignant tumors. The higher magnetic field strength may give benefits of potentially higher

**Correspondence to:**

Panyaping T. Department of Radiology, Ramathibodi Hospital, 270 Rama VI Road, Ratchathewi Bangkok, 10400, Thailand.  
**Phone:** +66-2-2011212, **Fax:** +66-2-2011297  
**Email:** theeraphol1@gmail.com

**How to cite this article:** Panyaping T, Wansophonkul S, Tuntiyatorn L. Role of diffusion-weighted MR imaging in differentiation of infectious spondylodiscitis and spinal malignancy. J Med Assoc Thai 2018;101:351-60.

signal-to-noise ratio, contrast-to-noise ratio, and spectral resolution for certain applications. We have proposed to compare ADC values between infectious spondylodiscitis and spinal malignant tumors on 3-T MRI, and to determine sensitivity, specificity, accuracy, positive predictive value [PPV], and negative predictive value [NPV] of using ADC value cutoff point for diagnosis of infectious spondylodiscitis.

## Materials and Methods

### Patient population

The patients with clinical suspicion for infectious spondylodiscitis or spinal malignant tumors were prospectively recruited from multidepartment of Ramathibodi Hospital between March 2015 and March 2016. Eighteen patients gave informed consent to perform pre-treatment MR images of the affected spine with diffusion-weighted technique. By the radiographic inclusion criteria, the patients were divided into two groups. The radiographic inclusion criteria of infectious spondylodiscitis are 1) hypointense T1/hyperintense T2 and/or enhancement on post-contrast T1 fat suppression [FS] images of vertebral bodies and/or intervening discs, and 2) erosion or destruction of one or more vertebral endplate(s), as shown in the Figure 1-3. The radiographic inclusion criteria of spinal malignant tumors are 1) hypointense T1/hyperintense T2 and/or enhancement on T1 FS post-contrast of vertebral bodies, and 2) relatively spared disc (no hyper T2 or enhancement), as seen on Figure 4 and 5. The diagnosis of infectious spondylodiscitis and spinal malignant tumors were later confirmed by either microbiological or histological studies or by clinical response to antimicrobial therapy (for infectious spondylodiscitis) or clinical response to radiation therapy or chemotherapy (for spinal malignant tumors). The patients who did not obtain pre-treatment MRI with diffusion-weighted technique, who had a prior spinal procedure, or who had no diagnostic confirmation with laboratory (microbiology or histopathology) or objective clinical evidence of response to antimicrobial therapy, radiotherapy, or chemotherapy, were excluded.

### MRI

All MR examinations were prospectively evaluated. They were performed on a 3-T MR system (Ingenia, Philips) by using corresponding multichannel torso coil. The standard protocol of pulse sequence parameters are sagittal T1-weighted spin echo<sup>(12)</sup>, pre- and post-contrast enhanced T1-weighted FS, T2-weighted turbo spin echo [TSE] and T2-weighted

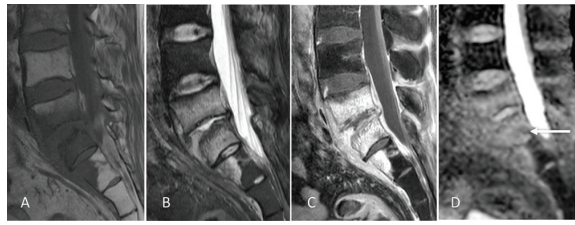


**Figure 1.** A 55-year-old man with streptococcus spondylodiscitis shows hypointense on T1W (A), hyperintense on T2W (B) with contrast enhancement (C) of L5 to S2 vertebral bodies and intervening L5/S1 disc with destruction of the vertebral endplates. On the ADC mapping, b-value of 800 seconds/mm<sup>2</sup> (D), the mean ADC at S1 lesion (arrow) is 1.753x10<sup>-3</sup> mm<sup>2</sup>/second.

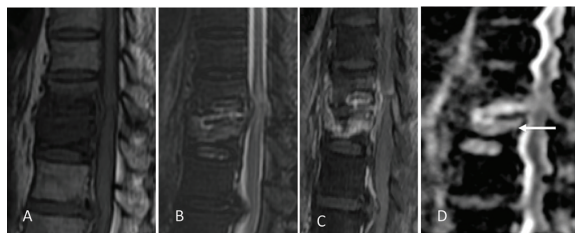


**Figure 2.** A 74-year-old woman with tuberculous spondylodiscitis shows hypointense on T1W (A), hyperintense on T2W (B) with contrast enhancement (C) of lower T10 and upper T11 vertebrae and intervening T10/11 disc, with destruction of the vertebral endplates. On the ADC mapping, b-value of 800 seconds/mm<sup>2</sup> (D), the mean ADC at T11 lesion (arrow) is 1.351x10<sup>-3</sup> mm<sup>2</sup>/second.

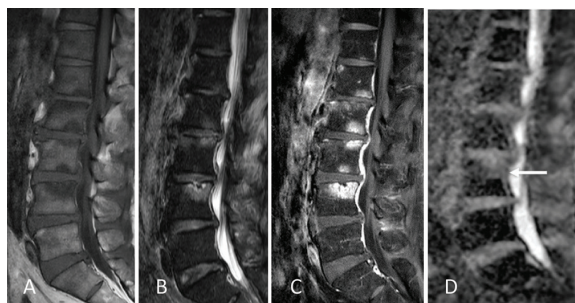


**Figure 3.** A 59-year-old woman with streptococcus suis spondylodiscitis shows multiple hypointense on T1W (A), hyperintense on T2W (B) with contrast enhancement (C) of L1 to L4 vertebrae with destruction of the vertebral endplates. On the ADC mapping, b-value of 800 seconds/mm<sup>2</sup> (D), the mean ADC at L4 lesion (arrow) is 1.375x10<sup>-3</sup> mm<sup>2</sup>/second.

FS, axial T1-weighted SE, T2-weighted FS, and post-contrast enhanced T1-weighted images, coronal T2-weighted fat suppression, and post-contrast enhanced T1-weighted images. DWI was performed as single shot TSE imaging on sagittal and axial planes with diffusion sensitivities, b-value = 400 seconds/mm<sup>2</sup> and

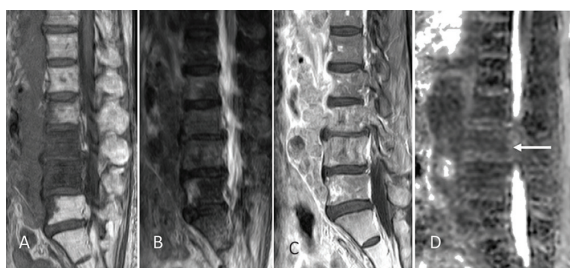


**Figure 4.** A 71-year-old woman with thyroid and cervical cancer with vertebral metastases, seen as hypointense on T1W (A), hyperintense on T2W (B) with contrast enhancement (C) of L2-L5 vertebral bodies, associated with prevertebral soft tissue masses, as well as central spinal canal extension. The intervertebral discs are relatively spared. On the ADC mapping, b-value of 800 seconds/mm<sup>2</sup> (D), the mean ADC at L4 lesion (arrow) is  $1.074 \times 10^{-3}$  mm<sup>2</sup>/second.

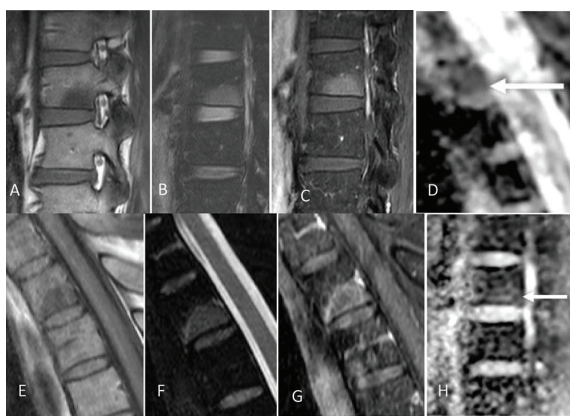


**Figure 5.** A 59-year-old man with lung cancer with vertebral metastases at the lower T2 (A-D) and L1 (E-H) vertebrae, seen as hypointense on T1W (A, E), hyperintense on T2W (B, F) with contrast enhancement (C, G). The intervertebral discs are preserved. On the ADC mapping, b-value of 800 seconds/mm<sup>2</sup> (D, H), the mean ADC at T2 and L1 lesions (arrows on D and H) is  $1.093 \times 10^{-3}$  mm<sup>2</sup>/second and  $0.879 \times 10^{-3}$  mm<sup>2</sup>/second, respectively.

800 seconds/mm<sup>2</sup>. The diffusion gradients were applied sequentially in three orthogonal directions to generate three sets of sagittal diffusion-weighted images. The repetition time/echo time [TR/TE] = 9,131/51 on sagittal plane, and TR/TE = 1,931/45 on axial plane, slice thickness, 4 mm, voxel, 2.5x2.5 mm, field of view [FOV] = 300 mm for sagittal plane and 200 mm for axial plane, 384x384 matrix, and SENSE 2 parallel imaging were used for all scans. The scanning time was 167 seconds. Two patients that received pre-treatment conventional computed tomography [CT] scan from an outside facility received additional DWI and sagittal T2-weighted short-tau inversion recovery [STIR]

images, TR/inversion time [TI]/TE = 4586/210/60, 256x256 matrix, voxel, 0.7x1.2 mm, 4-mm slice thickness, with 0.5-mm intersection gap, and FOV = 320 mm. Analysis of diffusion changes were performed by Extended MR Workspace 2.6.3.5, 2013, Philips medical systems Nederland B.V., Veenpluis 4-6, 5684 PC Best, The Netherlands, to calculate the ADC based on the Stejskal and Tanner equation<sup>(13)</sup> as the negative slope of the linear regression line best fitting the points for b versus ln (SI), where SI is the signal intensity from a region of interest [ROI] of the images acquired at the 3 b-values. The ADC maps were generated by automatically performing this calculation on a pixel-by-pixel basis. ROI measurements were defined on the sagittal ADC map. Each MRI study was evaluated by a neuroradiologist and a second-year neuroradiologic fellow trainee with consensus to include the cases with radiologic inclusion criteria of infectious spondylodiscitis and spinal malignant tumors. The reviewers understood that the patients had infectious spondylodiscitis or spinal malignant tumors, but were blinded to the final diagnosis. The ROI was drawn on sagittal ADC mapping (b = 400 and 800 seconds/mm<sup>2</sup>) by the second-year neuroradiologic fellow trainee<sup>(14)</sup> with consensus with the neuroradiologist, on the areas corresponding to enhancing marrow lesions on post-contrast T1-weighted FS and/or hyperintense T2 marrow lesions on T2W FS images (Figure 6). Each ROI was drawn lesion by lesion with at least 30 mm<sup>2</sup> in area. The ROIs were also drawn on the normal appearing marrow of the same MR study for control group. The software gave the measured quantitative parameters, i.e., the min ADC, mean ADC, max ADC, and standard deviation [SD]. Intraobserver ROI drawing was performed with 1-month interval.

### Statistical analysis

Statistical software (Stata version 14) was used for all data analysis. The mean ADC values of normal and abnormal bone marrow lesions (infectious spondylodiscitis and spinal malignant tumors) are shown in mean ± SD for normal distribution and median (P25 to P75) for non-normal distribution, and were compared using the Student's t-test for normal distribution, and Wilcoxon rank sum test for non-normal distribution. The min ADC, mean ADC, and max ADC of the infectious spondylodiscitis and spinal malignant tumors are shown in mean ± SD for normal distribution and median (P25 to P75) for non-normal distribution, and were compared using Student's t-test for normal distribution, and Wilcoxon

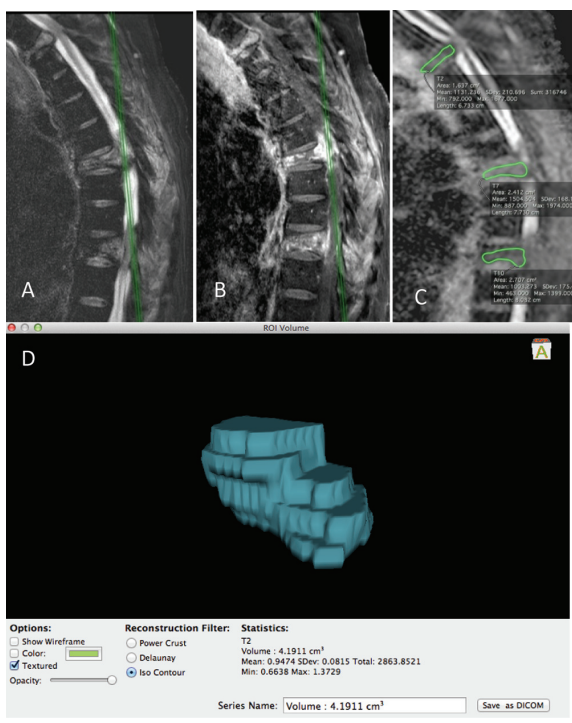


**Figure 6.** The ROI was drawn according to the hyperintense T2 or enhancing marrow lesions, using sagittal T2W FS (A) or post-contrast T1W FS (B) images as guide ROI encompassing on every sagittal cut of ADC mapping (C) to calculate volume, min ADC, mean ADC, max ADC, and SD.

rank sum test for non-normal distribution. Statistical significance was defined as  $p$ -value of less than 0.05. The intraobserver agreement was between at 1-month interval. Mean ADC measurements were calculated by using concordance correlation coefficient. The receiver operating characteristic [ROC] curve analysis was performed to find the mean ADC of the marrow lesion as a cutoff for diagnosis of infectious spondylodiscitis. Using this mean ADC cutoff, the sensitivity, specificity, accuracy, PPV, and NPV for diagnosis of infectious spondylodiscitis were calculated, using laboratory (microbiology, histology) diagnosis, or objective clinical evidence of response to antimicrobial therapy, radiotherapy, or chemotherapy as a gold standard. Intraobserver agreement of using mean ADC cutoff for diagnosis of spondylodiscitis was also calculated by k coefficient, which defined k values for level of agreement as follow: 0.81 to 0.99, almost perfect agreement; 0.61 to 0.80, substantial agreement; 0.41 to 0.60, moderate agreement; 0.21 to 0.40, fair agreement; and 0.01 to 0.20, slight agreement<sup>(15)</sup>. A Chi-square test or Fisher's exact test was used to compare the

categorical variables, and Wilcoxon-rank sum test was used for comparing continuous variables between infectious spondylodiscitis and spinal malignant tumors,  $p$ -value of less than 0.05 is considered statistically significant.

The estimate sample size for two-sample comparison of means, with power of 80%, and alpha of 0.05, according to the equation of

$$n = \frac{(Z_{\alpha/2} + Z_{\beta})^2 2xSD^2}{(\mu_1 - \mu_2)^2}$$

From the study of Pui et al<sup>(7)</sup> that compared ADCs between infectious spondylodiscitis and spinal malignancy. The mean ADC value of spinal malignancy is  $1.02 \pm 0.36 \times 10^{-3}$  mm<sup>2</sup>/second. The mean ADC value of spinal infectious group is expected to be higher than the spinal malignant group at least  $0.14 \times 10^{-3}$  mm<sup>2</sup>/second. The estimate sample size per group is 104, i.e., total estimate sample size of two groups is 208.

## Results

Between March 2015 and March 2016, 24 patients were acquired, but there were six patients with no laboratory (microbiology, histology) diagnosis, or objective clinical evidence of response to antimicrobial therapy, radiotherapy, or chemotherapy. Therefore, 18 patients who fulfilled the inclusion criteria were included and divided into two groups, eight patients (25 lesions, 47.17%) with infectious spondylodiscitis and 10 patients (28 lesions, 52.83%) with spinal malignant tumors. In the infectious spondylodiscitis group, the mean age was 64.8 years (age range 55 to 78 years) and included four men and four women. The diagnosis were confirmed by positive polymerase chain reaction [PCR] for *Mycobacterium tuberculosis* from the pleural fluid in two cases, positive hemoculture for *Streptococcus* group B in one case, positive hemoculture for *Streptococcus suis* in one case, and four cases with clinical suspicion for infectious spondylodiscitis with clinical improvement after antibiotic treatment (treatment duration range 58 to 62 days). In 25 infectious spondylodiscitis marrow lesions, the most common location was lumbar level (17 lesions, 68.0%), followed by cervical level (3 lesions, 12.0%), thoracic level (3 lesions, 12.0%) and sacrum (2 lesions, 8.0%). In the spinal malignant tumor group, the mean age was 58.5 years (age range 29 to 71 years) and included two men and eight women. The diagnosis was confirmed by spinal biopsy with pathologic diagnosis of metastatic carcinoma in five cases, osteosarcoma in one case, and four cases with known primary cancer with clinical improvement

(improved bone pain or improved bone marrow lesions) after radiation or chemotherapy. Nine patients with known primary cancer were four lung cancer patients, one case of base of tongue with oropharyngeal cancer, one patient with cancer of thyroid gland and cervix, two sigmoid cancer patients, and one renal cell carcinoma patient. In 28 spinal malignant marrow lesions, the most common location was thoracic level (20 lesions, 71.42%), followed by lumbar (6 lesions, 21.42%), and cervical (2 lesions, 7.14%) levels. The demographic data are shown in Table 1. There were no statistically significant differences in age and gender between these two groups.

All of the lesions in each group have MRI findings that were included in the radiographic inclusion criteria, which was infectious spondylodiscitis with 1) hypointense T1/hyperintense T2 and/or enhancement on post-contrast T1 FS of vertebral bodies and/or intervening disc, and 2) erosion or destruction of one or more vertebral endplate(s), spinal malignant tumors with 1) hypointense T1/hyperintense T2 and/or enhancement on T1 FS post-contrast of vertebral bodies, and 2) relatively spared disc (no hyper T2 signal or enhancement).

The mean ADC of control group was measured in the 47 normal appearing marrows from the same

MR study as the infectious spondylodiscitis and spinal malignant tumors. The mean ADC of the control group is statistically significant lower than the mean ADC of the abnormal marrow lesion group (infectious spondylodiscitis and spinal malignant tumors) on both b-values ( $b = 400$  and  $800$  seconds/mm<sup>2</sup>), as shown on Table 2.

The min ADC, mean ADC, max ADC on both b-values ( $b = 400$  and  $800$  seconds/mm<sup>2</sup>) of the infectious spondylodiscitis and spinal malignant tumors were compared (Table 3). Only mean ADC ( $b = 800$  seconds/mm<sup>2</sup>) of these groups showed statistically significant difference. The mean ADC of the infectious spondylodiscitis group ( $1.30 \pm 0.28 \times 10^{-3}$  mm<sup>2</sup>/second) was higher than that of the spinal malignant tumor group ( $1.10 \pm 0.20 \times 10^{-3}$  mm<sup>2</sup>/second). The mean ADC ( $b = 400$  seconds/mm<sup>2</sup>), min ADC, and max ADC ( $b = 400$  and  $800$  seconds/mm<sup>2</sup>) show no statistical significance between these groups.

ROC analysis was done to find the mean ADC ( $b = 800$  seconds/mm<sup>2</sup>) cutoff for diagnosis of infectious spondylodiscitis, with area under ROC curve of 0.7386 ( $p$ -value 0.01), and sensitivity and specificity as shown in Table 4. By using the mean ADC of the bone marrow lesion of  $1.116 \times 10^{-3}$  mm<sup>2</sup>/second and above as a cutoff for diagnosis of infectious spondylodiscitis, the sensitivity 75%, specificity 68%, accuracy 71.7%, PPV 72.4%, and NPV 70.8% with associated 95% confident interval are shown in Table 5. This mean ADC cutoff correctly categorized infectious spondylodiscitis 19 of 25 (75%) lesions. Alternatively, six of 25 (25%) lesions with infectious spondylodiscitis showed false negative. Nineteen of twenty-eight (68%) lesions with spinal malignant tumors were correctly classified, only nine of 28 (32%) lesions of spinal malignant tumors were misclassified as infectious spondylodiscitis. Figure 7 shows comparison of mean ADC between infectious spondylodiscitis and spinal malignant tumors by using mean ADC of  $1.116 \times 10^{-3}$  mm<sup>2</sup>/second and above as a cutoff for diagnosis of infectious spondylodiscitis.

**Table 1.** Demographic data

Characteristic	Infectious spondylodiscitis	Malignant tumors	<i>p</i> -value
Number, n (%)	25 (47.17)	28 (52.83)	
Age (years), mean $\pm$ SD	64.8 $\pm$ 8.35	58.5 $\pm$ 12.70	0.475
Range	55 to 78	29 to 71	
Gender, n (%)			0.321
Male	4 (50.00)	2 (20.00)	
Female	4 (50.00)	8 (80.00)	
Location, n (%)			
Cervical	3 (12.00)	2 (7.14)	
Thoracic	3 (12.00)	20 (71.43)	
Lumbar	17 (68.00)	6 (21.43)	
Sacrum	2 (8.00)	0 (0.00)	

**Table 2.** Mean apparent diffusion coefficient [ADC] values of abnormal marrow lesions (infectious spondylodiscitis and malignant tumor) and normal controls

Parameters	Abnormal marrow lesion (infectious spondylodiscitis and malignant tumor)	Normal controls	<i>p</i> -value
Number	53 (53%)	47 (47%)	
Mean ADC** ( $b = 400$ )	$1.18 (0.85 \text{ to } 1.48) \times 10^{-3}$	$0.65 (0.35 \text{ to } 0.98) \times 10^{-3}$	<0.001*
Mean ADC** ( $b = 800$ )	$1.21 \pm 0.27 \times 10^{-3}$	$0.54 \pm 0.24 \times 10^{-3}$	<0.001*

\* Statistically significant,  $p < 0.05$

\*\* The "Mean ADC" in this context means a parameter that measure from each abnormal marrow lesion or each normal control. The central tendency of the data set were shown in median (P25 to P75) for non-normal distribution of the "Mean ADC ( $b = 400$ )", and were shown in mean  $\pm$  SD for normal distribution of the "Mean ADC ( $b = 800$ )"

**Table 3.** ADC values of infectious spondylodiscitis and malignant tumors

Parameters	Infectious spondylodiscitis (n = 25)	Malignant tumors (n = 28)	p-value
1 <sup>st</sup> time (b = 400)			
Volume (cm <sup>3</sup> )	1.97 (0.52 to 6.54)	2.86 (2.03 to 5.10)	0.193
Mean ADC (mm <sup>2</sup> /second)	1.21±0.49 x10 <sup>-3</sup>	1.17±0.29 x10 <sup>-3</sup>	0.728
Min ADC (mm <sup>2</sup> /second)	0.34 (0.04 to 0.57) x10 <sup>-3</sup>	0.43 (0.24 to 0.65) x10 <sup>-3</sup>	0.549
Max ADC (mm <sup>2</sup> /second)	1.93 (1.56 to 2.67) x10 <sup>-3</sup>	2.45 (2.06 to 2.70) x10 <sup>-3</sup>	0.132
2 <sup>nd</sup> time (b = 400)			
Volume (cm <sup>3</sup> )	1.06 (0.27 to 2.28)	2.08 (0.58 to 2.71)	0.154
Mean ADC (mm <sup>2</sup> /second)	1.31±0.35 x10 <sup>-3</sup>	1.14±0.32 x10 <sup>-3</sup>	0.061
Min ADC (mm <sup>2</sup> /second)	0.62 (0.42 to 0.82) x10 <sup>-3</sup>	0.54 (0.40 to 0.79) x10 <sup>-3</sup>	0.605
Max ADC (mm <sup>2</sup> /second)	1.97±0.51 x10 <sup>-3</sup>	1.94±0.66 x10 <sup>-3</sup>	0.851
1 <sup>st</sup> time (b = 800)			
Volume (cm <sup>3</sup> )	2.40 (0.52 to 6.54)	2.86 (2.10 to 5.44)	0.247
Mean ADC (mm <sup>2</sup> /second)	1.30±0.28 x10 <sup>-3</sup>	1.10±0.20 x10 <sup>-3</sup>	0.004*
Min ADC (mm <sup>2</sup> /second)	0.57 (0.32 to 0.70) x10 <sup>-3</sup>	0.63 (0.49 to 0.70) x10 <sup>-3</sup>	0.769
Max ADC (mm <sup>2</sup> /second)	2.00±0.33 x10 <sup>-3</sup>	1.91±0.39 x10 <sup>-3</sup>	0.398
2 <sup>nd</sup> time (b = 800)			
Volume (cm <sup>3</sup> )	0.86 (0.23 to 2.28)	2.24 (0.74 to 2.80)	0.059
Mean ADC (mm <sup>2</sup> /second)	1.29±0.42 x10 <sup>-3</sup>	1.09±0.23 x10 <sup>-3</sup>	0.040*
Min ADC (mm <sup>2</sup> /second)	0.62±0.30 x10 <sup>-3</sup>	0.60±0.21 x10 <sup>-3</sup>	0.846
Max ADC (mm <sup>2</sup> /second)	1.89±0.52 x10 <sup>-3</sup>	1.67±0.41 x10 <sup>-3</sup>	0.093

\* Statistically significant, p<0.05

**Table 4.** ROC curve analysis of using mean ADC value (b = 800 seconds/mm<sup>2</sup>) for diagnosis of infectious spondylodiscitis

Cut point	Sensitivity	Specificity	LR+	LR-
≥1.007x10 <sup>-3</sup>	85.71%	32.00%	1.2605	0.4464
≥1.036x10 <sup>-3</sup>	85.71%	48.00%	1.6484	0.2976
≥1.116x10 <sup>-3</sup>	75.00%	68.00%	2.3438	0.3676
≥1.221x10 <sup>-3</sup>	60.71%	80.00%	3.0357	0.4911

**Table 5.** Using mean ADC of the bone marrow lesion of 1.116 x10<sup>-3</sup> mm<sup>2</sup>/second and above as a cutoff for diagnosis of infectious spondylodiscitis

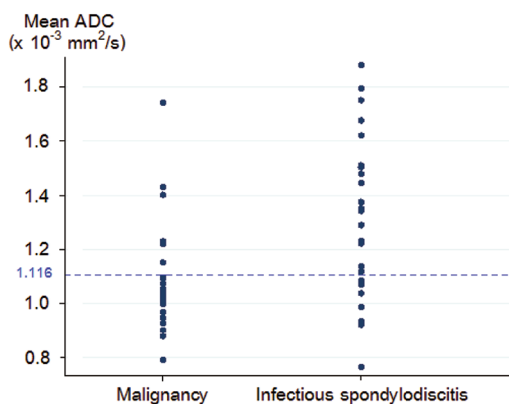
Characteristics	%	95% confidence interval
Sensitivity	75.0	55.1 to 89.3
Specificity	68.0	46.5 to 85.1
PPV	72.4	52.8 to 87.3
NPV	70.8	48.9 to 84.4

PPV = positive predictive value; NPV = negative predictive value

The intraobserver agreement of measuring mean ADC value (b = 800 seconds/mm<sup>2</sup>) at 1-month interval was evaluated using concordance correlation coefficient, with average = 0.011x10<sup>-3</sup> mm<sup>2</sup>/second, SD = 0.184x10<sup>-3</sup> mm<sup>2</sup>/second, 95% limits of agreement of mean ADC value between 0.350x10<sup>-3</sup> and 0.372x10<sup>-3</sup> mm<sup>2</sup>/second. By using kappa, the agreement between the intra-observer test of measuring mean ADC value (b = 800 seconds/mm<sup>2</sup>) at 1-month interval using 1.11x10<sup>-3</sup> mm<sup>2</sup>/second and above as cutoff for diagnosis of infectious spondylodiscitis by using the Cohen k statistics, there was a substantial agreement (k = 0.7325).

## Discussion

Infectious spondylodiscitis is characterized by involvement of two adjacent vertebrae and intervening disc with disc space narrowing, vertebral marrow edema, destruction of vertebral endplates, associated with prevertebral and epidural extension, abscess formation, and surrounding inflammatory tissue<sup>(7)</sup>. If not managed promptly, it can lead to poor outcome and hence early diagnosis is crucial. Sometimes, it is difficult to differentiate from malignant bone tumors. Although the presence of paraspinous abscess helps differentiate spinal infection from malignancy, the

**Figure 7.** Comparison of mean ADC between infectious spondylodiscitis and spinal malignant tumors by using mean ADC of 1.116x10<sup>-3</sup> mm<sup>2</sup>/second and above as a cutoff for diagnosis of infectious spondylodiscitis.

reactive marrow edema caused by tuberculosis and pyogenic infection may simulate diffuse hematologic malignancy and metastasis<sup>(16,17)</sup>.

Diffusion-weighted MR imaging derives benefit from the random mobility of water molecules to obtain information on the microscopic behavior of tissues<sup>(18)</sup>. The diffusion in bone marrow is related to the water molecules confined in marrow spaces defined by reticulum cells and fat cells. The degree of signal attenuation due to diffusion in a voxel, detected on a DWI sequence, is logarithmically dependent on the ADC of that voxel and the b-value. ADC is sensitive to cell volume fraction and cellularity in biologic tissues. The most useful diffusion-weighted echo planar imaging [EPI] technique is very sensitive to magnetic susceptibility effects, resulting in geometric distortion artifacts that tend to be more severe with increasing b-values. At first, we tried the b-value of 0, 400, 500, 600, 800, and 1,000 seconds/mm<sup>2</sup> on the MRI of the spine with EPI and TSE techniques, and then we found the optimized images that gave appropriate signal to noise ratio and less susceptibility artifact was that diffusion-weighted TSE pulse sequence with b-value of 400 and 800 seconds/mm<sup>2</sup>.

Basically, trabecular bone and fat cause structural tortuosity. If the trabecular and fat content is reduced in the bone marrow, there is less extracellular tortuosity and water diffusion is greater. Bone injury, infection, and tumor disrupt bone trabeculae and cause a local increase in water movement. However, in case of infiltrative marrow lesions, cellularity can be high, especially in actively growing malignant tumors resulting in restricted water diffusion in extracellular space. On the other hand, bone marrow edema results in higher extracellular volume fraction, which can occur in both neoplastic and infectious processes. In the present study, we supposed that spinal malignant tumors showed lower ADC due to predominant high cellularity, while higher ADC value in infectious spondylodiscitis was due to predominantly bone marrow edema.

There have been many previous studies using ADC value in differentiating benign and malignant spinal lesions. Chan et al<sup>(8)</sup> performed DWI on 1.5-T MRI with b-value of 1,000 seconds/mm<sup>2</sup> on patients with acute vertebral body compression. They reported the mean combined ADCs (ADCcmb; average of the combined ADCs in the x, y, and z diffusion directions) were  $0.23 \times 10^{-3}$  mm<sup>2</sup>/second in normal vertebrae,  $0.82 \times 10^{-3}$  mm<sup>2</sup>/second in malignant acute vertebral fractures and  $1.94 \times 10^{-3}$  mm<sup>2</sup>/second in benign acute

vertebral fractures, with statistically significant difference between ADCcmb values of the benign and malignant acute vertebral fractures without overlap, but some overlapping ADC values between malignant fractures and tuberculous spondylitis.

Herneth et al<sup>(10)</sup> evaluated the ADC in the assessment of vertebral metastases and acute vertebral compression fractures in 22 patients on 1-T MRI with b-value of 440 and 880 seconds/mm<sup>2</sup>. The ADCs in vertebral metastases ( $0.69 \times 10^{-3}$  mm<sup>2</sup>/second) and pathologic compression fractures ( $0.65 \times 10^{-3}$  mm<sup>2</sup>/second) can be safely distinguished from vertebral bodies ( $1.66 \times 10^{-3}$  mm<sup>2</sup>/second) and benign compression fractures ( $1.62 \times 10^{-3}$  mm<sup>2</sup>/second). The mean ADC of pathologic vertebral compression fractures was significantly lower than the ADC in benign vertebral compression fractures.

Maeda et al<sup>(11)</sup> studied the ADCs using 1.5-T MRI with b-value of 500 and 1,000 mm<sup>2</sup>/second in benign compression fractures ( $1.21 \pm 0.17 \times 10^{-3}$  mm<sup>2</sup>/second), malignant compression fractures ( $0.92 \pm 0.20 \times 10^{-3}$  mm<sup>2</sup>/second), and metastatic vertebral lesions without collapse ( $0.83 \pm 0.17 \times 10^{-3}$  mm<sup>2</sup>/second). The ADC was significantly higher in benign compression fractures than in malignant compression fractures, although the two types showed considerable overlap.

Balliu et al<sup>(19)</sup> performed 1.5-T DWI with b-value of 500 seconds/mm<sup>2</sup> and reported that acute malignant fractures were hyperintense compared to normal vertebral bodies on DWI, except in one patient with sclerotic metastases. Mean ADC value from benign edema ( $1.9 \pm 0.39 \times 10^{-3}$  mm<sup>2</sup>/second) was significantly higher than untreated metastatic lesions ( $0.9 \pm 1.3 \times 10^{-3}$  mm<sup>2</sup>/second). Mean ADC value of infectious spondylitis ( $0.96 \pm 0.49 \times 10^{-3}$  mm<sup>2</sup>/second) is not statistically different from untreated metastatic lesions. ADC value was low ( $0.75 \times 10^{-3}$  mm<sup>2</sup>/second) in one case of subacute benign fracture.

Only one previous study by Pui et al<sup>(7)</sup> compared ADCs between infectious spondylodiscitis and spinal malignancy like in our study. On 1.5-T diffusion-weighted MR imaging (b-value of 500 and 1,000 seconds/mm<sup>2</sup>) and using the ADC cutoff of  $1.02 \times 10^{-3}$  mm<sup>2</sup>/second for bone marrow, the sensitivity, specificity, and accuracy were 60.26%, 66.00%, and 62.50%, respectively, for distinguishing infectious spondylitis from spinal malignancy.

In our study, we found the statistically significant difference of mean ADC (b = 800 seconds/mm<sup>2</sup>) between infectious spondylodiscitis group ( $1.30 \pm 0.28 \times 10^{-3}$  mm<sup>2</sup>/second) and the spinal malignant tumor

group ( $1.10 \pm 0.20 \times 10^{-3} \text{ mm}^2/\text{second}$ ). Using mean ADC of the bone marrow lesion of  $1.116 \times 10^{-3} \text{ mm}^2/\text{second}$  and above as a cutoff for diagnosis of infectious spondylodiscitis, the sensitivity, 75%, specificity 68%, accuracy 71.7%, PPV 72.4%, and NPV 70.8%, were found higher than those from the previous study. This may be due to using higher field strength (3-T) that results in higher signal-to-noise ratio and contrast-to-noise ratio. In addition, the ROI in our study was drawn on every image in sagittal ADC mapping of the whole lesions that showed T2 hyperintensity or enhancement, but the study of Pui et al<sup>(7)</sup> placed the sampling ROI encompassing the largest area of highest SI in the abnormal bone marrow and any associated soft tissue mass, which may cause selection bias.

The ADC of normal marrow is different from the abnormal marrow lesions. Zhou et al<sup>(9)</sup> reported that benign compression fractures and metastatic lesions have lower ADC values than normal vertebral bodies when a b-value of 250 seconds/mm<sup>2</sup> was used. Similar to Chen et al<sup>(20)</sup>, the reported retrospective study of DWI on 1.5-T MRI with b-value of 400 and 800 seconds/mm<sup>2</sup> was that ADCs of the degenerative disc disease [DDD] and infectious spondylodiscitis groups were both significantly lower than that of the normal control group. However, we found that normal bone marrow showed that mean ADC was much lower than that in abnormal bone marrow. Our results agreed with those of previous reports in which higher b-values were used<sup>(8,21)</sup>.

The high ADC values of the malignancy may overlap with the infection. In our study only eight of 25 (32%) lesions of spinal malignant tumors were misclassified as infectious spondylodiscitis. The previous studies discussed the possible reasons for these results. First, necrotic tissues in malignant bone tumors could increase the ADC by increased extracellular volume fraction, as documented in a previous study<sup>(22)</sup>. However, there was no lesion with necrotic portion in our study. Second, a larger fraction of associated bone marrow edema might explain the high ADC in malignant compression fractures. Le Bihan<sup>(23)</sup> reported that in malignant compression fractures, a mixture of interstitial edema and malignant tumor cellularity occurred and might reduce the specificity of the diffusion analysis. Finally, the hypervascular portion of malignant tumors that increased the proportion of the perfusion effect might be responsible for the high ADC measurement results<sup>(24)</sup>.

Our study performed diffusion-weighted MR imaging on b-value of 400 and 800 seconds/mm<sup>2</sup>.

Only mean ADC on b-value of 800 seconds/mm<sup>2</sup> showed a statistically significant difference between the infectious spondylodiscitis and the spinal malignant tumors. ADC is more affected by perfusion in small b-values. Using a high b-value of 800 seconds/mm<sup>2</sup> helps minimize the perfusion effect. High b-value and T2 weighting can also increase the sensitivity of diffusion imaging to movement.

There are several limitations in our study. First, we collect the cases prospectively in only 1-year interval, resulting in small sample size. There are too few patients for subgroup analysis in each pathogen of infectious spondylodiscitis. Second, only four cases of the infectious spondylodiscitis group and six cases from the spinal malignant tumor group have a positive microbiologic diagnosis, or pathologic confirmation, respectively. The remaining cases were diagnosed by clinical improvement after treatment. Third, the single-shot TSE imaging had poor temporal resolution and was sensitive to motion artifact. At first, we did both single-shot TSE and single-shot EPI to compare the image quality, and found that the single-shot TSE had better signal-to-noise ratio, less susceptibility artifact, less geometric distortion, but trade off with minimally loss contrast resolution. However, DWI must be sensitive to molecular motion in the order of 10  $\mu\text{m}$ , and sensitive to bulk tissue motion including blood flow, swallowing, and respiratory motion leading to ghosting artifact. This was most apparent in the cervical and upper thoracic spine. With the recent system and software innovations, these problems can be partially overcome by using phased array spine coil, more acquisitions, and multi-shot EPI with cardiac gating, navigator echoes, or regional saturation slab.

In conclusion, our study showed that the mean ADC could have role for significantly differentiating infectious spondylodiscitis from spinal malignant tumors, using 3-T MRI, DWI TSE with b-value 800 seconds/mm<sup>2</sup>, although there might be some overlap of the mean ADC between these two groups.

## Conclusion

Diffusion-weighted MR imaging has role in differentiating between infectious spondylodiscitis and spinal malignant tumors, especially when imaging findings on conventional images are inconclusive.

## What is already known on this topic?

There have been many previous studies using ADC value in differentiating benign and malignant spinal lesions. However, there has been only one study



comparing ADCs between infectious spondylodiscitis and spinal malignancy on 1.5-T MRI. Spinal malignant tumors showed lower ADC due to predominant high cellularity, while higher ADC value in infectious spondylodiscitis due to predominantly bone marrow edema.

### What this study adds?

The present study showed significantly higher ADC values of the infectious spondylodiscitis than those of the spinal malignant tumors on 3-T MRI. We found higher sensitivity, specificity, and accuracy for diagnosis of infectious spondylodiscitis than that from the previous study by using mean ADC of the bone marrow lesion of  $1.116 \times 10^{-3}$  mm<sup>2</sup>/second and above as a cutoff point. This may be due to using higher field strength (3T) that results in higher signal-to-noise ratio and contrast-to-noise ratio.

### Potential conflicts of interest

The authors declare no conflict of interest.

### References

1. Tsiodras S, Falagas ME. Clinical assessment and medical treatment of spine infections. *Clin Orthop Relat Res* 2006;444:38-50.
2. Butler JS, Shelly MJ, Timlin M, Powderly WG, O'Byrne JM. Nontuberculous pyogenic spinal infection in adults: a 12-year experience from a tertiary referral center. *Spine (Phila Pa 1976)* 2006;31:2695-700.
3. Cottle L, Riordan T. Infectious spondylodiscitis. *J Infect* 2008;56:401-12.
4. Maiuri F, Iaconetta G, Gallicchio B, Manto A, Briganti F. Spondylodiscitis. Clinical and magnetic resonance diagnosis. *Spine (Phila Pa 1976)* 1997;22:1741-6.
5. Thurnher MM, Bammer R. Diffusion-weighted magnetic resonance imaging of the spine and spinal cord. *Semin Roentgenol* 2006;41:294-311.
6. Pongpornsup S, Wajanawichakorn P, Danchaiwijit N. Benign versus malignant compression fracture: a diagnostic accuracy of magnetic resonance imaging. *J Med Assoc Thai* 2009;92:64-72.
7. Pui MH, Mitha A, Rae WI, Corr P. Diffusion-weighted magnetic resonance imaging of spinal infection and malignancy. *J Neuroimaging* 2005;15:164-70.
8. Chan JH, Peh WC, Tsui EY, Chau LF, Cheung KK, Chan KB, et al. Acute vertebral body compression fractures: discrimination between benign and malignant causes using apparent diffusion coefficients. *Br J Radiol* 2002;75:207-14.
9. Zhou XJ, Leeds NE, McKinnon GC, Kumar AJ. Characterization of benign and metastatic vertebral compression fractures with quantitative diffusion MR imaging. *AJNR Am J Neuroradiol* 2002;23:165-70.
10. Herneth AM, Friedrich K, Weidekamm C, Schibany N, Krestan C, Czerny C, et al. Diffusion weighted imaging of bone marrow pathologies. *Eur J Radiol* 2005;55:74-83.
11. Maeda M, Sakuma H, Maier SE, Takeda K. Quantitative assessment of diffusion abnormalities in benign and malignant vertebral compression fractures by line scan diffusion-weighted imaging. *AJR Am J Roentgenol* 2003;181:1203-9.
12. Raya JG, Dietrich O, Reiser MF, Baur-Melnyk A. Techniques for diffusion-weighted imaging of bone marrow. *Eur J Radiol* 2005;55:64-73.
13. Westin CF, Maier SE, Mamata H, Nabavi A, Jolesz FA, Kikinis R. Processing and visualization for diffusion tensor MRI. *Med Image Anal* 2002;6:93-108.
14. Williams RL, Fukui MB, Meltzer CC, Swarnkar A, Johnson DW, Welch W. Fungal spinal osteomyelitis in the immunocompromised patient: MR findings in three cases. *AJNR Am J Neuroradiol* 1999;20:381-5.
15. Viera AJ, Garrett JM. Understanding interobserver agreement: the kappa statistic. *Fam Med* 2005;37:360-3.
16. Tonziello G, Valentinotti R, Stacul F, Giacomazzi D, Luzzati R. Spinal lesions by infectious spondylodiscitis and hepatocellular carcinoma presenting as spinal metastasis in an HIV-HCV co-infected patient. *Infez Med* 2015;23:187-91.
17. Gupta RK, Agarwal P, Rastogi H, Kumar S, Phadke RV, Krishnani N. Problems in distinguishing spinal tuberculosis from neoplasia on MRI. *Neuroradiology* 1996;38 (Suppl 1):S97-104.
18. Hagmann P, Jonasson L, Maeder P, Thiran JP, Wedeen VJ, Meuli R. Understanding diffusion MR imaging techniques: from scalar diffusion-weighted imaging to diffusion tensor imaging and beyond. *Radiographics* 2006;26 (Suppl 1):S205-23.
19. Balliu E, Vilanova JC, Pelaez I, Puig J, Remollo S, Barcelo C, et al. Diagnostic value of apparent diffusion coefficients to differentiate benign from malignant vertebral bone marrow lesions. *Eur J Radiol* 2009;69:560-6.

20. Chen TY, Wu TC, Tsui YK, Chen HH, Lin CJ, Lee HJ, et al. Diffusion-weighted magnetic resonance imaging and apparent diffusion coefficient mapping for diagnosing infectious spondylodiscitis: a preliminary study. *J Neuroimaging* 2015;25:482-7.
21. Byun WM, Shin SO, Chang Y, Lee SJ, Finsterbusch J, Frahm J. Diffusion-weighted MR imaging of metastatic disease of the spine: assessment of response to therapy. *AJNR Am J Neuroradiol* 2002;23:906-12.
22. Lang P, Wendland MF, Saeed M, Gindele A, Rosenau W, Mathur A, et al. Osteogenic sarcoma: noninvasive in vivo assessment of tumor necrosis with diffusion-weighted MR imaging. *Radiology* 1998;206:227-35.
23. Le Bihan DJ. Differentiation of benign versus pathologic compression fractures with diffusion-weighted MR imaging: a closer step toward the "holy grail" of tissue characterization? *Radiology* 1998;207:305-7.
24. van Rijswijk CS, Kunz P, Hogendoorn PC, Taminiau AH, Doornbos J, Bloem JL. Diffusion-weighted MRI in the characterization of soft-tissue tumors. *J Magn Reson Imaging* 2002;15:302-7.